

# Analysis of Mach-Zehnder OADM Characteristics using Fiber Bragg Gratings

P. T. Neves Jr., F. Kuller, C. Marconcin, H. J. Kalinowski, J. L. Fabris and A. A. P. Pohl.

**Abstract**—An add/drop based in a all fiber Mach-Zehnder interferometer and two identical fiber Bragg gratings (MZ-FG) assembled with discrete components is investigated with experiment and simulation. The influence of the components parameters on undesirable power return is showed.

**Index Terms**—Fiber Bragg Gratings, optical fiber devices, optical add/drop.

## I. INTRODUCTION

THE add/drop based in a all fiber Mach-Zehnder interferometer and two identical fiber Bragg gratings (MZ-FG) was originally described by [1]. An OADM performance based in MZ-FG devices was demonstrated for the first time in a six-channel 10 Gbit/s experiment in [2] verifying excellent features of the MZ-FG.

As shown in Fig.1, for a WDM system with  $n$  channel, an add/drop unit cell for  $\lambda_i$  can be implemented using two 3dB couplers and two fiber Bragg gratings with  $\lambda_i$  as the Bragg wavelength. For ideal performance, if couplers, gratings and interferometer arms are balanced, the  $\lambda_i$  channel is reflected by the gratings and directed to Drop port instead to the Input port due to double  $\pi/2$  phase shift arising at the 3dB coupler [3]. Due to the same reason, the  $\lambda_i$  channel applied on Add port is directed to the Output port. Remaining channels are not affected by the device.

Multiplexing and demultiplexing can occur at the same time in the same device without crosstalk between multiplexed and demultiplexed signals if the reflectivity of the Bragg grating is infinitely high. In practice reflectivity above than 99% is required [4].

After the assembling process the optical path of the interferometer's arms usually show a small difference. This difference must be compensated to ensure a perfect phase match on couplers avoiding power return to Input and Add ports. It can be done with a UV trimming on each side of one of the grating [4] exposing one arm of the interferometer to

uniform UV light in order to photoinduce an average index change in the fiber core.

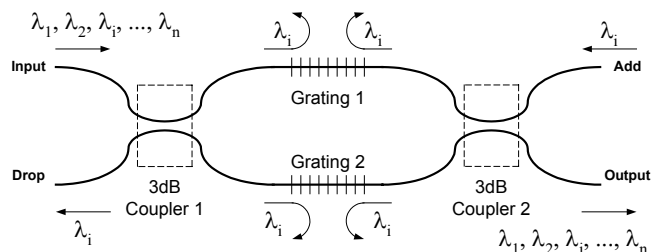


Fig. 1. Unit cell schematic for an Add/drop MZ-FG

With the purpose of studying the impact of not ideal components on the device behavior, we used in this work an unbalanced interferometer, without UV trimming, with slightly mismatched low reflectivity fiber gratings and couplers with different coupling ratios. We show the influence of each parameter on the undesirable power return.

## II. METHODOLOGY

### A. Experiment

An add/drop filter made with a Mach-Zehnder interferometer and two almost identical fiber grating was assembled, as shown in Fig.1. Gratings 1 and 2 were fabricated at CEFET-PR [5] and have Bragg wavelengths at 1536.88nm and 1536.48nm, respectively. Both show 12 dB rejection and 0.5 dB bandwidth. Coupler 1 and 2 have coupling ratios of 0.51 and 0.48, respectively. A three port circulator with 0.4 dB insertion loss was inserted at the Input port in order to measure the optical power returned to it.

To test the device a superluminescent LED with center wavelength emission at 1544.2 nm and FWHM = 58.8 nm was used at the Input port. The measured spectrum of the source is shown in Fig. 2. Reflected and transmitted spectra were measured on the Drop and Output ports, respectively. No signal was applied at the Add port..

Authors are with the Centro Federal de Educaço Tecnolgica do Paran (CEFET-PR), Av. Sete de Setembro, 3165, 80230-901, Curitiba – PR, Brazil (corresponding author: phone: +55-41-3104735; e-mail: pohl@cpgei.cefetpr.br).

This work received financial support from Conselho Nacional de Desenvolvimento Científico e Tecnolgico (process CNPq 473.454/2003-3) and from the GIGA project, supported by FUNTEL/FINEP. P. Neves Jr. thanks Coordenaço de Aperfeiçoamento de Pessoal de Nível Superior (CAPES) for the research scholarship.

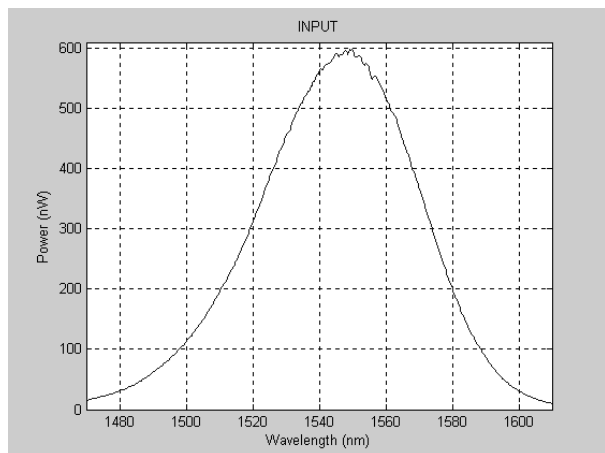


Fig. 2. Spectrum of the LED source viewed by the Optical Spectrum Analyzer using 1 nm resolution.

As a further attempt to avoid the returned power to the device Input port an axial strain was applied on Grating 2. Since the gratings do not show exactly the same Bragg wavelength, this step is necessary to provide adjustment of the reflected wavelength on both gratings. After the matching attempt, the same measurements were performed in all ports.

### B. Simulation

The software VPItransmissionMaker™ was used on the simulation of the device. To simulate the LED signal, a Gaussian pulse with Gaussian Order = 1, Emission Frequency = 194.275 THz (1544.2 nm), Peak Power = 180 mW and FWHM = 59.692 fs (58.8 nm) was used. The spectrum of such pulse demonstrates a good concordance between the experimental source (LED) and the simulation source.

The system showed in Fig. 1 (adding the circulator) was implemented in the simulation with the real characteristics of the gratings, couplers and circulator used in the experiment, including the insertion loss of each device. Also, simulations were done for the ideal case, where the coupling factor of both couplers is 0.5 and gratings characteristics are identical (same bandwidth).

## III. RESULTS

### A. Simulation for the Ideal Case

Setting the system balanced (coupling ratio of 0.5, gratings with the same insertion loss, Bragg wavelength, bandwidth and rejection), no power returns to the ports Input Return and Add. All the power filtered by the gratings goes to the Drop port and the remaining power go ahead to the Output port.

### B. Simulation with Unbalanced Coupling Factor

Setting the coupling ratio at 0.51 and 0.48 for Coupler 1 and Coupler 2, respectively, and keeping the gratings identical and the ideal circulator, a small fraction of power returns to Input port, as shown in Fig. 3. Note that the Power axis is in dBm. Small differences on the coupling factor do not affect

expressively the device performance.

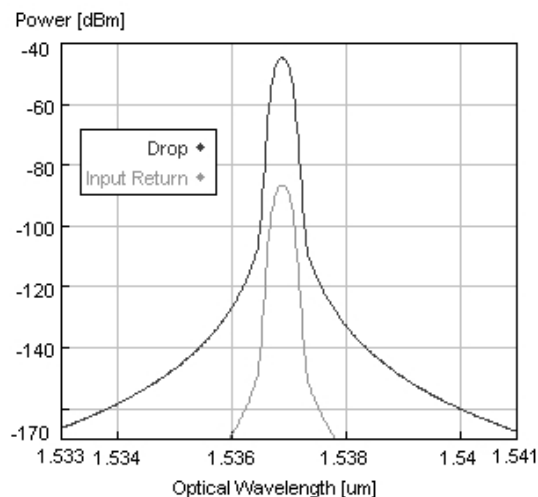


Fig. 3. Drop and Input Return spectra for unbalanced coupling factor (resolution = 0.1 nm).

### C. Simulation with Unbalanced Bragg Wavelengths

In this case the Bragg wavelength was set at 1536.88 nm and 1536.48 nm for Grating 1 and Grating 2, respectively, whereas the coupling ratio factor was kept at 0.5 for both couplers.

As shown in Fig. 4, the amount of power on Drop and Input Return ports is almost the same. However, simulations show that any Bragg wavelength variation in the gratings cause reflection power to be split between the Input port and Add port.

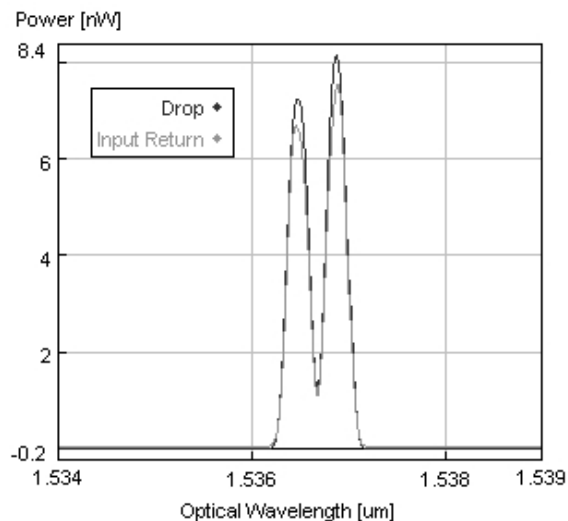


Fig. 4. Drop and Input Return spectra for unbalanced gratings concerning the Bragg wavelength (resolution = 0.1 nm).

### D. Comparison Between Experimental and Simulated Results.

The real MZ-FG device shows couplers and gratings with unbalanced characteristics. Fig. 5 and Fig. 6 show the

experimental and simulated results, respectively. Difference in Power axis is due to the fact that the LED does not have a perfect gaussian spectrum.

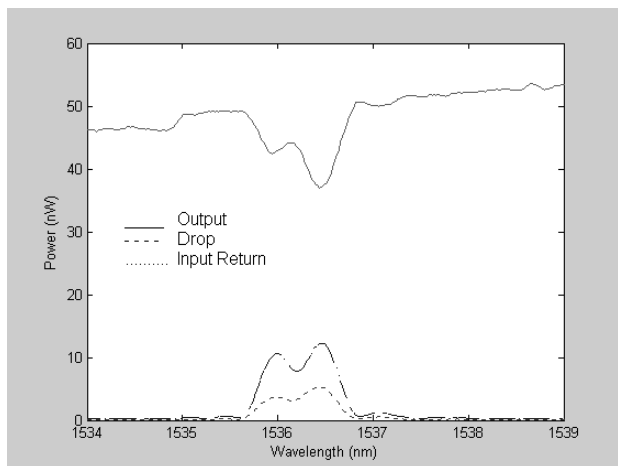


Fig. 5. Experimental Output, Drop and Input Return spectra for unbalanced gratings and couplers (resolution = 0.1 nm).

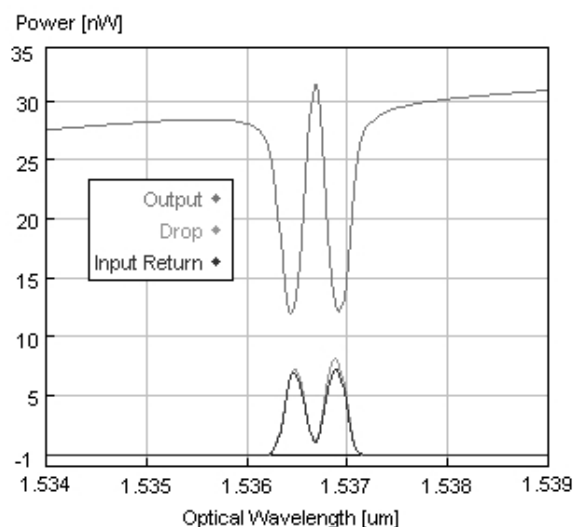


Fig. 6. Simulated Output, Drop and Input Return spectra for unbalanced gratings and couplers (resolution = 0.1 nm).

An axial strain was experimentally applied on Grating 2 in order to shift the Bragg wavelength, making it identical to Grating 1. Experimental and simulated results for this case are shown in Fig. 7 and Fig. 8, respectively, with the Power axis in linear scale. One should note that in the simulated result the Input Return power is negligible, as opposed to the experimental result. This happens due to the unbalanced interferometer arms. Since no UV trimming or other phase compensation technique was used, some amount of power is reflected to the Input Return port in the real device.

The optical path added by the matching of the Bragg wavelengths is often not the same one needed to compensate the unbalanced arms of the couplers.

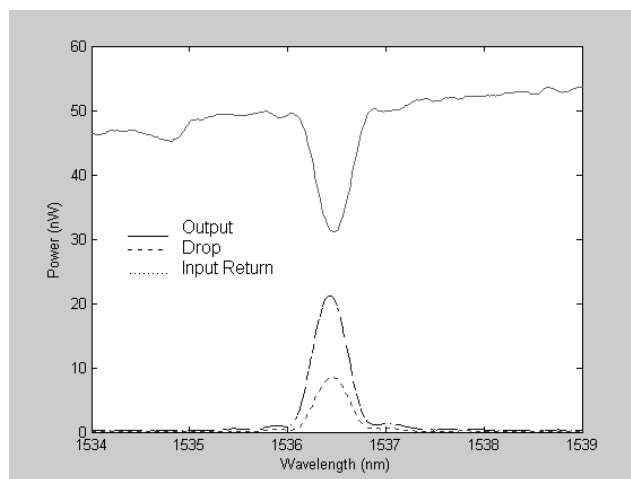


Fig. 7. Experimental Output, Drop and Input Return spectra for balanced gratings and unbalanced couplers (resolution = 0.1 nm).

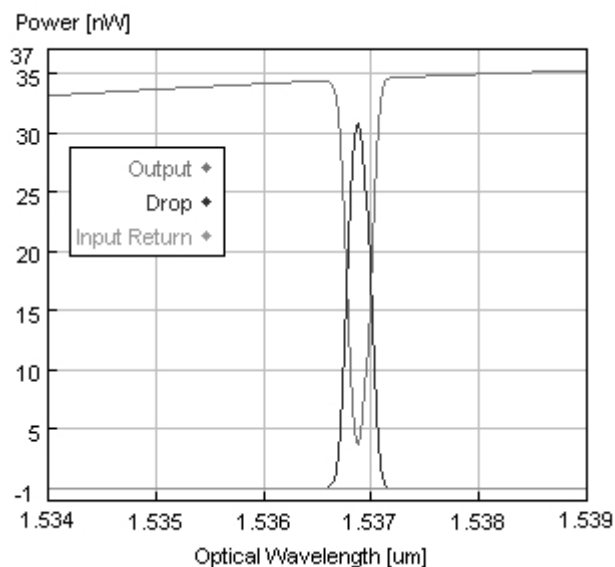


Fig. 8. Simulated Output, Drop and Input Return spectra for balanced gratings and unbalanced couplers (resolution = 0.1 nm).

#### IV. CONCLUSION

This work shows that small differences in the coupling ratios of ordinary, real couplers, do not affect expressively the device performance, as long as the Bragg wavelength on both gratings coincide. However, balanced interferometer arms are critical to a good work because the phase match on couplers is imperative. For narrow-band characteristic, the gratings must be fabricated with Bragg wavelength as identical as possible to avoid power returns. Although this all-fiber device presents lower cost and low losses, its assembly with real, discrete devices requires attention in order to avoid undue return power to the input and add ports.

## REFERENCES

- [1] D. C. Johnson, K. O. Hill, F. Bilodeau, S. Faucher, "New design concept for a narrow band wavelength-selective optical tap and combiner," *Electron. Lett.*, vol. 23, pp. 668–669, 1987.
- [2] T. Mizuochi, K. Shimizu, and T. Kitayama, "All-fiber add/drop multiplexing of 6 x 10 Gbit/s using a photo-induced Bragg grating filter for WDM networks," in *Tech. Dig. OFC '96*, San Jose, CA, Feb. 1996, paper WF2.
- [3] W. W. Morey, "Tunable narrow-line bandpass filter using fiber gratings," in *Tech. Dig. OFC '91*, San Diego, CA, Feb. 1991, paper PD-20.
- [4] F. Bilodeau, D. C. Johnson, S. Thériault, B. Malo, J. Albert, and K. O. Hill, and, "An all-fiber dense-wavelength-division Multiplexer / Demultiplexer using photoimprinted Bragg gratings," *IEEE Photon. Technol. Lett.*, vol. 7, pp. 388–390, Apr. 1995.
- [5] J. C. Cardoso da Silva, I. Abbe, R. C. Chaves, J. L. Fabris, J. L. Pinto, H. J. Kalinowski, C. L. Barbosa, "Development of Bragg grating sensors at CEFET-PR," *Optics and Lasers in Engineering*, vol. 39, pp. 511–523, 2003.